V. Dzhagan[1,2], O. Kapush[1], S. Budzulyak[1], N. Mazur[1], Ye. Havryliuk[1], A. Litvinchuk[3], S. Kondratenko[2], V. Yukhymchuk[1], M. Valakh[1]

Colloidal Cu₂ZnSnS₄-Based and Ag-Doped Nanocrystals: Synthesis and Raman Spectroscopy Study

[1]*V. Lashkaryov Institute of Semiconductors Physics, National Academy of Sciences of Ukraine, Kyiv, Ukraine, buser@ukr.net*
[2]*Taras Shevchenko National University of Kyiv, Kyiv, Ukraine, kondratenko@ukr.net*
[3]*Texas Center for Superconductivity and Department of Physics, University of Houston, Houston, USA, litvin@central.uh.edu*

Cu₂ZnSnS₄ (CZTS) is one of the promising materials for absorber layers of new-generation thin film solar cells. Various synthetic routes of materials preparation and structural characterization have been explored so far. Further tuning of the CZTS properties is realized via partial substitution of the cations. Here we have used an affordable and scalable method of synthesizing colloidal CZTS nanocrystals (NC) in an aqueous solution. Variation of the synthesis parameters, in particular pH of the solution, was employed to improve the crystallinity of the NCs. Furthermore, CZTS NCs with partial substitution of Cu for Ag were also successfully synthesized. Raman spectroscopy was employed as a prime tool of structural characterization of the NCs obtained, along with optical absorption spectroscopy and *ab initio* DFT lattice dynamics calculations. An experimentally observed slight upward shift of the main phonon Raman peak upon increase of the Ag content in $(Ag_xCu_{1-x})_2ZnSnS_4$ NCs is in agreement with the trend predicted by DFT calculation. No pure Ag_2ZnSnS_4 NCs could be formed, indicating a critical role of Cu in forming the kesterite structure NCs under given synthesis conditions in an aqueous medium.

Keywords: CZTS, nanocrystals, colloidal solution, Raman spectroscopy, phonons, DFT, solar cells.

Introduction

In view of an ever-growing depend on electricity, shrinkage of the carbon-based fossil fuel deposits and increasing environmental concerns, research on alternative energy sources based on nanomaterials expands [1-3]. The family of direct bandgap semiconductors like Cu₂ZnSnS₄ is considered to be one of the promising absorber materials for the next-generation photovoltaics, due to earth-abundant and non-toxic constituents, as wells as appropriately high coefficient of solar light absorption ($\sim 10^4$ cm⁻¹) [4]. This material allows the reduction of absorber layer thickness by at least a factor of 100, compared to today's Si ones, offering a possibility to significantly reduce manufacturing costs and enable fabrication on flexible substrates [5]. Delayed commercialization of Cu₂ZnSnS₄-based solar cells is primarily due to their relatively low

efficiency, around 13 % [6]. The underlying limitation is known to be physical in nature and caused by low formation energy of Zn_{Cu}, Cu_{Zn}, V_{Cu} point defects, and their complexes. These defects are responsible for a tail of the density of states near the energy bands and concomitantly reduced open circuit voltage (V_{OC}). As a possible solution for overcoming this problem a partial substitution of Cu^+ and Zn^{2+} with ions of different ionic radius and preferential coordination has been recently discussed [7]. In particular, numerous reports have shown an improved lattice (cationic) order upon a partial Cu for Ag substitution, as well as a concomitant increase of the solar cell efficiency [7-9] or photocatalytic efficiency [10], although negative effects of the substitution have been reported as well [11]. Notably, a dramatic broadening of the Raman and/or XRD peak with Ag content increase in the latter publication was observed for highly perfect NC lattice seen by TEM [11]. Moreover, embedding Ag into CZTS above certain

content switches conductivity to *n*-type [9]. For $(Cu_{1-x}Ag_x)_2ZnSn(S,Se)_4$ with high Ag content the stannite structure seems to be more favorable than kesterite, that is more common for CZTS [10]. In other published reports on NCs, a transition from wurtzite to kesterite structure was observed at Ag content around 0.3 [11]. Unlike CZTS nanocrystals (NCs), AZTS NCs can be fluorescent [12], with the radiative recombination being an undesirable competing recombination channel in PV devices. Therefore, the cationic substitutions can bring both new opportunities and challenges, which may manifest themselves differently for material obtained by different routes. One of the promising routes to obtain a thin absorber layer, especially for flexible PV, is a synthesis of NC of a desired composition in a colloidal solution [13], with subsequent deposition of the NC layer on the (flexible) substrate by printing, spin- or spray-coating, or other technique [5].

Raman spectroscopy is an established characterization technique for CZTS and many related compounds, including colloidal NPs [14-23]. It is capable of detecting secondary (impurity) phases [15, 24], and is not demanding to the amount of the material and its special preparation for the measurement, unlike XRD and TEM, and can probe NCs even in as-synthesized solutions. Most Raman studies of CAZTS and AZTS were performed so far on poly-/microcrystalline samples [25-30], with much fewer reports for NC samples [11, 12, 31]. However, even in microcrystalline and single crystals samples, the assignment of the Raman spectra to either kesterite or stannite structure is ambiguous or even contradictory. For instance, part of published reports on AZTS identifies the underlying structure as stannite based on the position of Raman peak located at 340-345 cm⁻¹ and referring (by analogy) to the works that observed a similar peak position for kesterite AZTS [29]. Furthermore, there is a noticeable discrepancy in the literature regarding the phonon Raman peaks position and width as a function of the Ag content in CAZTS, NC size, or deviation from stoichiometry (i.e. from I₂-II-IV-VI₄ formula) [8, 30]. With the growing number of reports on the synthesis and applications of colloidal CAZTS and other CZTS-like NCs [11, 12, 31-33] , both the phonon Raman spectra and structural phases in such NCs need to be further systematically explored.

Therefore, Raman spectroscopy was chosen in this work as a main characterization tool of the CZTS and cation-substituted NCs synthesized by means of an affordable and non-toxic route in aqueous media. The experimental optical and lattice dynamics results are supported by *ab initio* DFT calculations.

I.   Experimental

Materials. Thioglycolic acid (TGA), CuCl₂ × 2·H₂O, SnCl₂ × 2H₂O, Zn(CH₃COO)₂ × 2H₂O, NaOH, Na₂S × 9H₂O, AgNO₃, 2-propanol were supplied by Sigma Aldrich. All these chemicals were used as received. All glassware was cleaned with aqua regia (3:1 v/v HCl (37 %) :HNO₃ (65 %) solutions) and then rinsed thoroughly with deionized water (DI water) before use. Caution: aqua regia solutions are dangerous and should be used with extreme care; never store these solutions in closed containers. Deionized water (18 MΩ cm, Millipore) was used to prepare all solutions in the experiments.

Synthesis of CAZTS NCs. Colloidal CAZTS NCs were obtained by low temperature colloidal synthesis in the Erlenmeyer flask with continuous mixing in the presence of TGA as a stabilizer according to the procedure described previously in [33]. As the dispersion medium deionized water was used.

A stock aqueous 0.5 M solution of SnCl₂ in 4.0 M NaOH was prepared by slowly pouring an aqueous 1.0 M suspension of SnCl₂ × 2H2O into an aqueous 8.0 M solution of NaOH (volume ratio of the suspension and NaOH solutions were 1:1) and were of 24 hours left at room temperature.

Colloidal CAZTS NCs were synthesized in a reaction between a mixture of TGA complexes of Cu²⁺, Zn²⁺, and Sn²⁺ and sodium sulfide in deionized water. In a typical synthesis, (0.6 –x) mL aqueous 1.0 M CuCl₂ solution, x mL aqueous 1.0 M AgNO₃ solution (x = 1 - 100 %), 0.6 mL aqueous 0.5 M SnCl₂ with 4.0 M NaOH solution and 0.3 mL aqueous 1.0 M Zn(CH₃COO)₂ solution were consecutively added to 16 mL deionized water under stirring followed by the addition of 0,44 mL TGA and 0.05 - 0,7 mL aqueous 8.0 M NaOH solution. Finally, 0.6 mL aqueous 1.0 M Na₂S solution was added. The synthesis was complete when the color of the suspension no longer changed. Typically, the reaction took 30 - 60 sec.

Our study showed that obtained solutions along with NCs contain stabilizer excess, Cl⁻, CH₃COO²⁻ ions and (depending on the ratio of initial compounds) Na⁺, Cu²⁺, Zn²⁺, and Sn²⁺ ions. Taking into account that CZTS and CAZTS NCs obtained by this procedure have a charge on the surface, the ions present in the system can interact with NCs surface. To decrease the effect of nature and number of precursors on stability and the optical properties of obtained colloidal solutions, we developed a procedure for recovery of NCs from initial solutions by a selective precipitation method similar to the one in our previous reports on NCs CdTe [34]. For this purpose, equimolar volumes of initial solution and 2-propanol were mixed in a glass cylinder and kept for 1 min at room temperature under constant stirring. Flocculation of particles occurs because TGA-stabilized NCs are insoluble in 2-propanol. When a lesser amount of 2-propanol is added, no flocculation is observed, while an excess of 2-propanol degrades the thioglycolate shell of NC and therefore solution loses sedimentation stability. The obtained mixture was centrifuged for 1-5 min at a rate of 2000 – 10000 rpm. The obtained flocculant was separated from the mother liquor by decantation, washed many times with 2-propanol, and peptized in deionized water.

Characterization. Raman spectra were excited with a 532 nm or 671 nm single-longitudinal-mode solid-state lasers, with a power density on the samples of less than 10³ W/cm², which was low enough to preclude any thermal or photo-induced modification of the sample. Dispersion of the spectra was performed using a single-stage spectrometer (MDR-23, LOMO) with a spectral
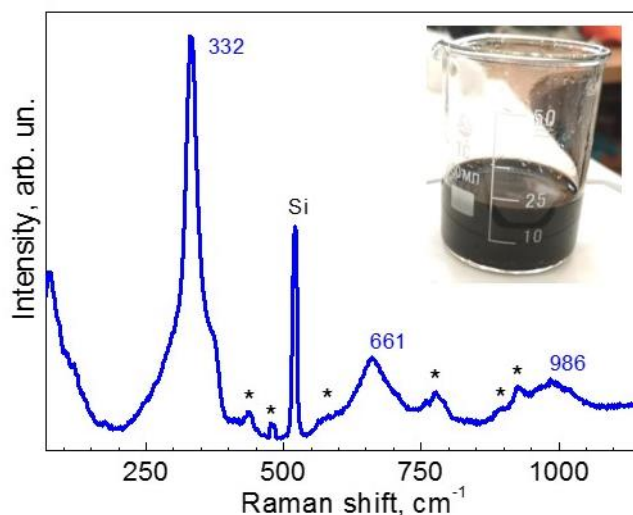
Fig. 1. Representative Raman spectrum of the CZTS NCs (λ_{exc} = 532 nm). The strongest phonon peak (A-symmetry mode, 332 cm^{-1}) that is characteristic of the kesterite structure of the NCs and corresponding second-order (at 661 cm^{-1}) and third-order (at 986 cm^{-1}) phonon process are marked. Minor features denoted by asterisks are Raman peaks that do not belong to the NCs and are related with by-products of the synthesis.

resolution of 6 cm^{-1} (as measured by the peak width of single crystal Si substrate and Rayleigh peak). Detection of the spectra was performed with TE-cooled (- 60 °C) CCD detector (Andor iDus 420). At least 4 spots were probed in each sample studied, in order to ensure that the sample is homogeneous and the obtained spectra are representative of the sample. Optical absorption spectra were recorded from NC solutions using the StellarNet Silver Nova 25 BWI6 Spectrometer.

Lattice dynamics calculations. *Ab-initio* linear response (density functional perturbation theory) lattice dynamics calculations of both CZTS and AZTS were performed within the generalized gradient approximation using the Perdew-Burke-Ernzerhof local functional [35] and as implemented in the CASTEP code [36]. Norm-conserving pseudopotentials were used. Before performing calculations the structures were relaxed while keeping lattice parameters fixed and equal to the experimentally determined ones so that forces on atoms in the equilibrium position did not exceed 2 meV/°A and the residual stress was below 0.01 GPa. A self-consistent field (SCF) tolerance better than 10^{-7} and a phonon SCF threshold of 10^{-12} were imposed. For calculations of the electronic ground state an integration within the Brillouin zone was performed over a 3×3×4 Monkhorst-Pack grid [37] in reciprocal space. As it is known, such an approach is proven to provide reliable results for quaternary semiconducting materials with various crystallographic structures [38,39]

II. Results and discussion

Figure 1 shows a representative Raman spectrum of CZTS NCs at λ_{exc} = 532 nm that is resonant for CZTS and potential secondary phases of Cu$_x$S and Cu$_x$Sn$_y$ [15, 19]. All the major peaks can be assigned to kesterite CZTS, in particular, the characteristic first-order peak at 332 cm^{-1} of (A$_1$ symmetry to S vibration around Sn with

the cations at rest) and corresponding higher-order phonon scattering peaks at 658 and 995 cm^{-1} [40-42]. Noteworthy is the relatively small full width at half maximum (FWHM) of the A$_1$ peak, 20 cm^{-1}, which is comparable to that of microcrystalline CZTS films and NCs synthesized in organic solvents at high temperatures (250 - 300 °C) [43-47]. Along with observing the higher-order phonon features, it indicates a good crystallinity of these CZTS NCs synthesized under rather mild conditions in the water. From the frequency position of the main Raman mode at 332 cm^{-1} we can assume that CZTS NCs possess the so-called cation-disordered kesterite structure [42, 48, 49].

It is further worth noting that CZTS NCs synthesized under mild conditions possess not only good crystallinity of the targeted quaternary compound, but reveal also the absence of spectral traces of any possible secondary phase – Cu$_x$S (470 cm^{-1}), Cu$_x$SnS$_y$ (317 cm^{-1}), SnS (310 cm^{-1}).

Different parameters of the synthesis can be used to optimize the crystallinity and other parameters of the semiconductor NCs obtained in colloidal solutions. For the aqueous synthesis approach used in this work, some of the key parameters have already been optimized in the initial work that had introduced this way of synthesis [33]. Here we have investigated the influence of an important parameter that was not studied earlier, in particular, the pH of the solution. Figure 2 shows Raman spectra of CZTS NCs synthesized at various pH between 3.5 and 11, acquired with λ_{exc} = 532 nm (a) and λ_{exc} = 671 nm (b). It can be seen that over entire pH range the Raman spectra possess the characteristic kesterite mode, although of a varied intensity.

The intensity values normalized to the intensity of the Si substrate, which compensates for the different film thickness in different samples, is plotted in Fig. 3. One can notice a certain variation of both the peak intensity and position, which can be indicative of the dependence of the internal structure of the NCs on the pH value of
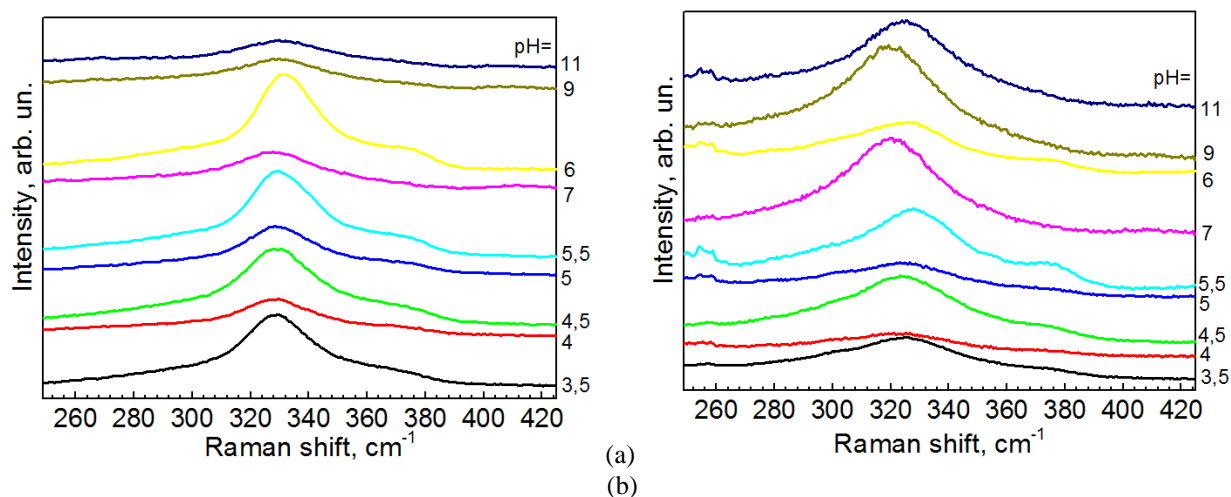
Fig. 2. Raman spectra of the series of CZTS NCs synthesized at different pH (from 3.5 to 11) acquired with λ_{exc}=532 nm (a) and λ_{exc}=671 nm (b). Only the range of the main phonon peak is shown for better visibility of spectral position of the peak maximum: rather constant for λ_{exc}=532 nm and variable for λ_{exc}=671 nm. See text for the discussion of this effect.
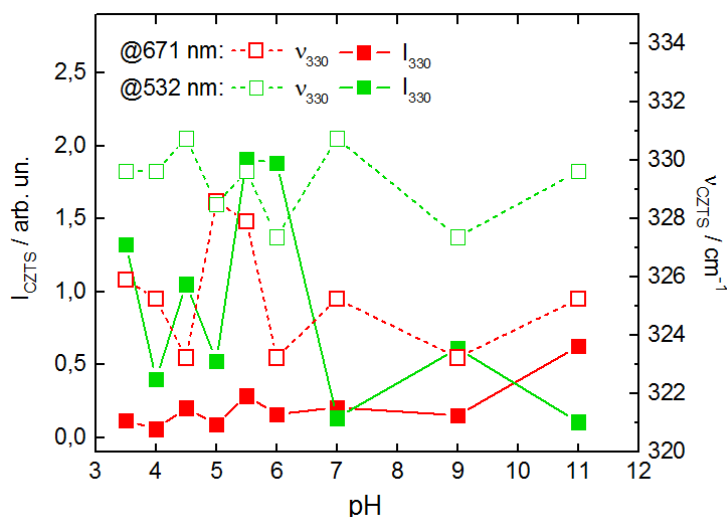

Fig. 3. Raman peak intensity (solid lines and filled symbols) and frequency position (dashed lines and open symbols) of the main phonon mode of the CZTS NCs obtained at different pH. The data for λ_{exc}=532 nm (green) and λ_{exc}=671 nm (red) are presented.

the medium. Note that there was no noticeable variation of the Raman spectrum parameters observed within the samples, as concluded from measuring at least four different points on each sample.

An obvious observation that can be made from Fig. 3 is a lower frequency of the phonon peak at the red (671 nm) excitation. This could be due to the selectivity of the particular λ_{exc} to NCs with the closest bandgap value, while the different phonon frequencies at different λ_{exc} may indicate the bandgap distribution due to NC size variation of NCs with different composition. Apparently, these effects need to be addressed in more detail in future studies.

As mentioned in the introduction, one of the promising ways of tuning the structural and other properties of the CZTS-like NCs is (a partial) substitution of the constituent elements. In the present work, we have synthesized and studied the series of $(Ag_xCu_{1-x})_2ZnSnS_4$ (ACZTS) NCs with nominal Ag content x varied from 0 % to 15 %. Figure 4a shows the Raman spectra of this series of samples in the broad spectral range, which all contain the discussed above characteristic peaks of the kesterite CZTS structure.

From Fig. 4b one can see only a small upward shift of the main phonon peak with increased Ag content. This result is in agreement with some literature reports [8, 50], although a downward shift was reported by others [51] [11, 30]. What both groups of reports have in common is the small difference in the peak position compared to the CZTS one. This can be explained by the fact that the most intense (A₁-mode) peak is due to a symmetric vibration of anion without involving any cation motion. The modes that involve cation vibration are not resolved in the present work, but in studies where it was observed as a separate peak, it exhibited a continuous shift toward the low energy side with Ag content increase, well
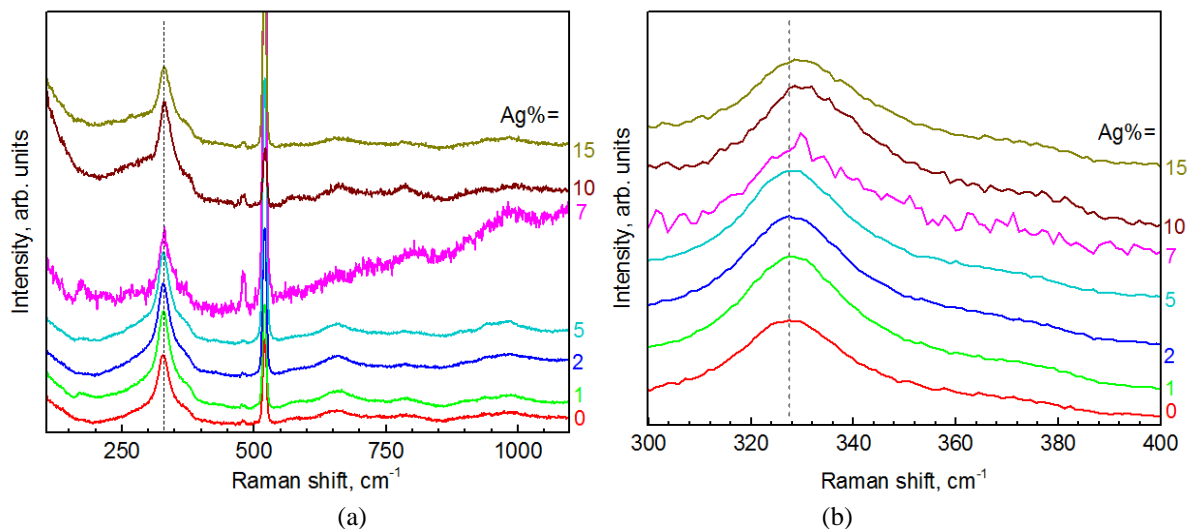
(a)   (b)

Fig. 4. Raman spectra (λ_{exc} = 532 nm) of a series of $(Ag_xCu_{1-x})_2ZnSnS_4$ (ACZTS) NCs with nominal Ag content x between 0 % and 15 %. The broad spectra range encompassing first, second, and third order phonon features is shown in (a). The first-order phonon spectra are shown in (b) to demonstrate the dependence of the peak position *vs*. Ag content.

Table 1

Calculated frequencies (in cm^{-1}) of phonon modes of CZTS and ACZTS of kesterite modification. The mode marked with an asterisk (338 for CZTS and 353 for AZTS) corresponds to the strongest peak observed in the experimental spectra

CZTS kesterite				AZTS kesterite	
A	B	E	A	B	E
279	64	72	239	50	61
285	74	96	268	83	89
338*	166	158	353*	155	139
	251	268		217	220
	315	287		300	276
	350	343		367	355

reflecting the effect of the substitution of Cu^+ by the heavier and bigger Ag^+ [50]. Consequently, most of the works on ACZTS nano- or microcrystals have reported main Raman peak around the same frequency as for CZTS ones, 332 - 338 cm^{-1} [31, 27], although some authors reported the main Raman peak at 345 - 348 cm^{-1} [28, 29, 32] (mostly without a clear statement about the type of crystal structure). The latter most likely were indicating the formation of stannite AZTS, as can be concluded from the only existing Raman study of a single crystal AZTS [26], which can be used as a reference. Despite the high crystallinity and large NC size (~20 nm), neither XRD nor TEM was able to prove the (kesterite or stannite) structure in Ref. [32]. Our *ab initio* DFT calculations of the phonon spectrum of kesterite AZTS show the main phonon (A_1-mode) frequency to be by 14 cm^{-1} higher than that of the kesterite CZTS (Table 1). Although a certain deviation of the phonon frequency between the experiment and calculation is acceptable, in this case, the rather noticeable difference can be because calculation was performed for pure AZTS (i.e. 100 % of Ag) while the

highest (nominal) Ag content achieved and measured in the experiment was 50 % (see below). Moreover, the lower phonon frequency in the experimental spectrum can be due to cation disorder, well established for CZTS, which is not accounted for in calculations.

Noteworthy is that introduction of Ag into the lattice can lead to reduction of a certain structural inhomogeneity inside NCs, as can be concluded from a much smaller variation of the phonon peak position in the series of CAZTS NCs (Fig. 5) as compared to CZTS NCs (Fig. 3).

The mild and affordable synthesis route used in this work allows relatively high concentrations of Ag to be introduced into the CAZTS lattice, as can be seen from the sharp phonon Raman peak of the samples synthesized with a nominal ratio of Ag:Cu = 1:1 (Fig. 6, two upper curves). However, our experiment with synthesizing purely AZTS NCs (i.e. without Cu) was not successful (Fig. 6, two lower curves). This experiment demonstrates the crucial role of Cu ions in forming the stable kesterite lattice in the aqueous environment.

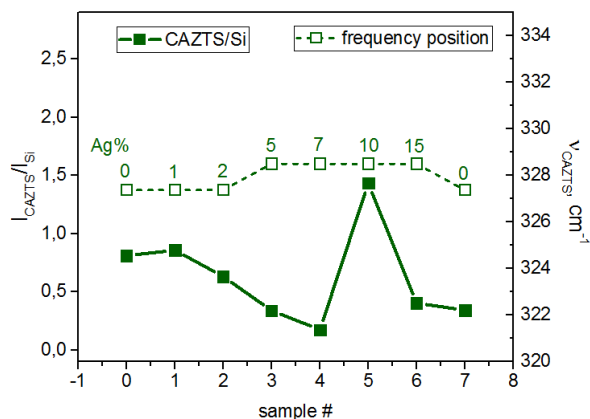An important characteristic of the material that is

Fig. 5. Raman peak intensity (solid lines and filled symbols) and frequency position (dashed lines and open symbols) of the main phonon mode (derived from the spectra in Fig. 5) of the CAZTS NCs with a nominal composition of Ag varied from 0 to 15 %.

considered for application as a light-absorbing layer of a solar cell is its optical absorption spectrum. Figure 7 shows the spectra of the pH-series of CZTS NCs discussed above. Although most of the spectra extend deeply into the red spectral range, some of the samples have particularly strong absorption in the red range and thus can be considered as more promising from the viewpoint of application. Even though both AZTS and CZTS are direct bandgap compounds, the absorption edge of such materials is always rather "smeared". The same typical lineshape possess also CZTS (Fig. 7a) and ACZTS NPs (Fig. 7b) in this work. The absence of a distinct absorption edge is attributed to the Urbach tail formed by a high density of the gap states [41], which are present even in the samples with high crystallinity in terms of XRD or TEM data [12]. The different contribution of certain defect states to this absorption tail may account for a scatter of the literature results and non-monotonous behavior of the CZTS and AZTS band gap value as a function of NCs size or Ag content (in the CAZTS). In particular, E_g of 1.48 - 1.65 eV was reported

for highly crystalline 5 - 7 nm AZTS NCs in [12], which is ~0.5 eV below the band gap of the bulk Ag₂ZnSnS₄, 2.0 eV. Note that despite a very crystalline TEM picture, both the Raman and XRD peaks of the NCs in Ref. [12] were very broad, particularly the Raman peak width much broader than that of the NCs in the present work.

No significant change or non-monotonous variation of the band gap value of the CAZTS NPs within a noticeable range of Ag content has been reported also in other works [9-11, 50-53].

We have investigated the effect of purification of the as-synthesized NC solution on the Raman spectrum. The standard purification step (described in detail in the experimental section) consisted of precipitation of the
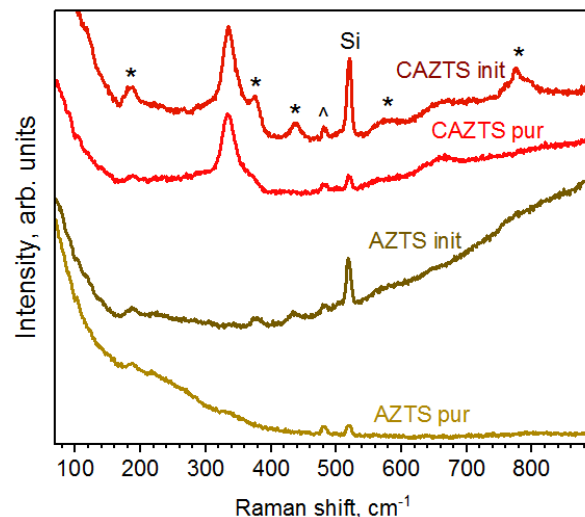

Fig. 6. Raman spectra (λ_{exc} = 532 nm) of as-synthesized (init) CAZTS NCs with nominal ratio Ag/Cu = 1 and AZTS NCs and the same NCs after purification (pur). The peaks marked with asterisks (*) are from by-products of the synthesis, which are visibly decreased in intensity after purification. The peak originating from the Si substrate used for depositing the NCs for Raman measurements (Si) and room light peak (^) are also marked.
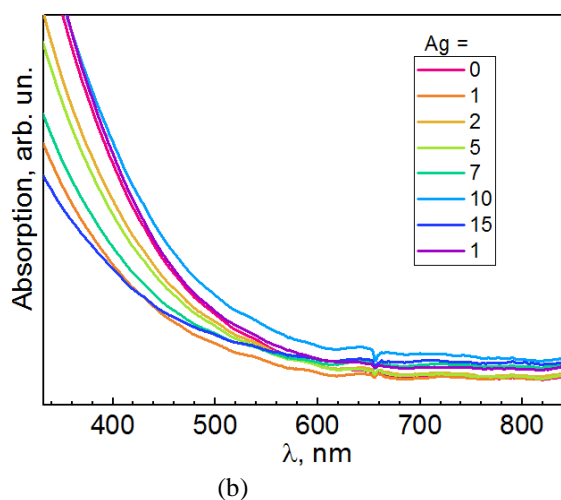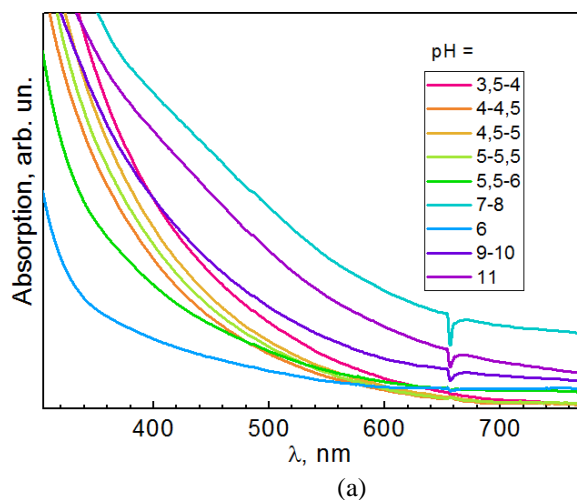

(a)

(b)

Fig. 7. Optical absorption spectra of the CZTS NCs obtained at different pH (a) and CAZTS NCs with different Ag content (b).

NCs by adding a bad solvent (isopropanol) with subsequent centrifugation, and re-dispersion of the precipitate in water. The spectrum of the CZTS sample that has been subject to such a purification reveals a significant suppression of the features (*) not related with the NCs (Fig. 7). At the same time, the peaks related with NCs are not affected by the purification procedure, indicating that the NCs obtained with the present synthesis route do not very different size fractions of CZTS phase, which would otherwise be separated by centrifugation.

Conclusions

An affordable and scalable method of synthesizing colloidal CZTS NCs in an aqueous solution is proposed, which allows to produce single phase NC material with a distinct vibrational Raman fingerprint of the kesterite CZTS structure. Notably, no spectral features of any secondary phase were detected. Variation of the synthesis parameters, in particular pH of the solution, was employed to improve the crystallinity of the NCs. Furthermore, CZTS NCs with partial substitution of Cu for Ag were also successfully synthesized. An experimentally observed slight upward shift of the main phonon Raman peak with an increase of the Ag content in $(Ag_xCu_{1-x})_2ZnSnS_4$ NCs agrees with the trend predicted by DFT calculation. No pure Ag_2ZnSnS_4 NCs could be formed, indicating a critical role of Cu in forming the kesterite structure under given synthesis conditions.

Dzhagan V. – Doctor of Physical and Mathematical Sciences;
Kapush O. – Ph.D;
Budzulyak S. – Ph.D;
Mazur N. – Master of Sciences;
Havryliuk Ye. – Ph.D;
Litvinchuk A. – Doctor of Physical and Mathematical Sciences;
Kondratenko S. – Professor, Doctor of Physical and Mathematical Sciences;
Yukhymchuk V. – Professor, Doctor of Physical and Mathematical Sciences;
Valakh M. – Professor, Doctor of Physical and Mathematical Sciences.

[1] B. Zhang, J. Sun, U. Salahuddin, P. Gao, Nano Futur. 4, 012002 (2020).

[2] O. Stroyuk, Springer, Cham, 2018 (https://doi.org/10.1007/978-3-319-68879-4).

[3] A.I. Kachmar, V.M. Boichuk, I.M. Budzulyak, O. Volodymyr, B.I. Rachiy, R.P. Lisovskiy, et al., Fullerenes, Nanotub. Carbon Nanostructures 27, 669 (2019) (https://doi.org/10.1080/1536383X.2019.1618840).

[4] H. Zhou, W. Hsu, H. Duan, B. Bob, W. Yang, Energy Environ. Sci. 6, 2822 (2013) (https://doi.org/10.1039/c3ee41627e).

[5] V.A. Akhavan, B.W. Goodfellow, M.G. Panthani, C. Steinhagen, T.B. Harvey, C.J. Stolle, et al., J. Solid State Chem. 189, 2 (2012) (https://doi.org/10.1016/j.jssc.2011.11.002).

[6] S. Giraldo, Z. Jehl, M. Placidi, V. Izquierdo-roca, A. Pérez-rodríguez, E. Saucedo, Adv. Mater. 1806692 (2019) (https://doi.org/10.1002/adma.201806692).

[7] Y.E. Romanyuk, S.G. Haass, S. Giraldo, M. Placidi, D. Tiwari, D.J. Fermin, et al., J. Phys. Energy 1, 044004 (2019) (https://doi.org/10.1088/2515-7655/ab23bc).

[8] X. Yu, S. Cheng, Q. Yan, J. Yu, W. Qiu, Z. Zhou, et al., RSC Adv. 8, 27686 (2018) (https://doi.org/10.1039/C8RA04958K).

[9] X. Liang, P. Wang, B. Huang, Q. Zhang, Z. Wang, Y. Liu, et al., ChemPhotoChem. 811 (2018) (https://doi.org/10.1002/cptc.201800109).

[10] I. Tsuji, Y. Shimodaira, H. Kato, H. Kobayashi, A. Kudo, Chem. Mater. 22, 1402 (2010) (https://doi.org/10.1021/cm9022024).

[11] N. Liu, F. Xu, Y. Zhu, Y. Hu, G. Liu, L. Wu, et al., J. Mater. Sci Mater. Electron. 31, 5760 (2020) (https://doi.org/10.1007/s10854-020-03146-8).

[12] A. Saha, A. Figueroba, G. Konstantatos, Chem. Mater. 32, 2148 (2020) (https://doi.org/10.1021/acs.chemmater.9b05370).

[13] O. Stroyuk, A. Raevskaya, N. Gaponik, Chem. Soc. Rev. 47, 5354 (2018) (https://doi.org/10.1039/c8cs00029h).

[14] M. Dimitrievska, A. Fairbrother, X. Fontané, T. Jawhari, V. Izquierdo-Roca, E. Saucedo, et al., Appl. Phys. Lett. 104, 021901 (2014) (https://doi.org/10.1063/1.4861593).

[15] Y. Havryliuk, M.Y. Valakh, V. Dzhagan, O. Greshchuk, V. Yukhymchuk, A. Raevskaya, et al., RSC Adv. 8, 30736 (2018) (https://doi.org/10.1039/C8RA05390A).

[16] M. Guc, A.P. Litvinchuk, S. Levcenko, M.Y. Valakh, I. V. Bodnar, V.M. Dzhagan, et al., RSC Adv. 6, 13278 (2016) (https://doi.org/10.1039/C5RA26844C).

[17] J.F.L. Lox, Z. Dang, V.M. Dzhagan, D. Spittel, B. Martín-García, I. Moreels, et al., Chem. Mater. 30, 2607 (2018) (https://doi.org/10.1021/acs.chemmater.7b05187).

[18] J. Li, B. Kempken, V. Dzhagan, D.R.T. Zahn, J. Grzelak, S. Mackowski, et al., CrystEngComm. 17, 5634 (2015) (https://doi.org/10.1039/C5CE00380F).

[19] V.V Brus, I.S. Babichuk, I.G. Orletskyi, P.D. Maryanchuk, V.O. Yukhymchuk, V.M. Dzhagan, et al., Appl. Opt. 55, B158 (2016) (https://doi.org/10.1364/AO.55.00B158).

[20] G. Gurieva, D.M. Többens, M.Y. Valakh, S. Schorr, J. Phys. Chem. Solids. 99, 100 (2016) (https://doi.org/10.1016/j.jpcs.2016.08.017).

[21] V. Dzhagan, B. Kempken, M. Valakh, J. Parisi, J. Kolny-Olesiak, D.R.T. Zahn, Appl. Surf. Sci. 395, 24 (2017) (https://doi.org/10.1016/j.apsusc.2016.08.063).

[22] V.M. Dzhagan, Y.M. Azhniuk, A.G. Milekhin, D.R.T. Zahn, J. Phys. D Appl. Phys. 51, 503001 (2018) (https://doi.org/10.1088/1361-6463/aada5c).

[23] V.V. Strelchuk, S.I. Budzulyak, I.M. Budzulyak, R.V. Ilnytsyy, V.O. Kotsyubynskyy, M.Ya. Segin, L.S.Yablon, Semicond. Physics, Quantum Electron. Optoelectron. 13, 309 (2010) (https://doi.org/10.15407/spqeo13.03).

[24] O. Selyshchev, Y. Havryliuk, M.Y. Valakh, V.O. Yukhymchuk, O. Raievska, O.L. Stroyuk, et al., ACS Appl. Nano Mater. 3, 5706 (2020) (https://doi.org/10.1021/acsanm.0c00910).

[25] K. Cheng, S. Hong, ACS Appl. Mater. Interfaces. 10, 22130 (2018) (https://doi.org/10.1021/acsami.8b04849).

[26] K. Pietak, C. Jastrzebski, K. Zberecki, D.J. Jastrzebski, W. Paszkowicz, S. Podsiadlo, J. Solid State Chem. 290, 121467 (2020) (https://doi.org/10.1016/j.jssc.2020.121467).

[27] A. Nagaoka, K. Yoshino, K. Kakimoto, K. Nishioka, J. Cryst. Growth. 555, 125967 (2021) (https://doi.org/10.1016/j.jcrysgro.2020.125967).

[28] J. Kumar, S. Ingole, J. Alloy. Compd. 865, 158113 (2021) (https://doi.org/10.1016/j.jallcom.2020.158113).

[29] L. Qiu, J. Xu, Nanomaterials 9, 1520 (2019) (https://doi.org/10.3390/nano9111520).

[30] V.A. Online, K. Timmo, M. Altosaar, M. Pilvet, V. Mikli, M. Grossberg, et al., J. Mater. Chem. A. 7, 24281 (2019) (https://doi.org/10.1039/c9ta07768e).

[31] X. Chen, J. Wang, W. Zhou, Z. Chang, D. Kou, Z. Zhou, et al., Mater. Lett. 181, 317 (2016) (https://doi.org/10.1016/j.matlet.2016.06.037).

[32] X. Hu, S. Pritchett-Montavon, C. Handwerker, R. Agrawal, J. Mater. Res. 4, 3810 (2019) (https://doi.org/10.1557/jmr.2019.328).

[33] O. Stroyuk, A. Raevskaya, O. Selyshchev, V. Dzhagan, N. Gaponik, D.R.T. Zahn, et al., Sci. Rep. 8, 13677 (2018) (https://doi.org/10.1038/s41598-018-32004-1).

[34] O.A. Kapush, L.I. Trishchuk, V.N. Tomashik, Z.F. Tomashik, S.D. Boruk, J. Inorg. Chem. 58, 1166 (2013) (https://doi.org/10.1134/S0036023613100124).

[35] J.P. Perdew, K. Burke, M. Ernzerhof, Phys. Rev. Lett. 77, 3865 (1996) (https://doi.org/10.1103/PhysRevLett.77.3865).

[36] S.J. Clark, M.D. Segall, C.J. Pickard, P.J. Hasnip, M.J. Probert, K.Z. Refson, et al., Z. Krist. 220, 567 (2005) (https://doi.org/10.1524/zkri.220.5.567.65075).

[37] H.J. Monkhorst, J.D. Pack, Phys. Rev. B. 13, 5188 (1976) (https://doi.org/10.1103/PhysRevB.13.5188).

[38] A.P. Litvinchuk, V.M. Dzhagan, V.O. Yukhymchuk, M.Y. Valakh, I.S. Babichuk, O. V. Parasyuk, et al., Phys. Rev. B. 90, 165201 (2014) (https://doi.org/10.1103/PhysRevB.90.165201).

[39] M. Dimitrievska, F. Boero, A.P. Litvinchuk, S. Delsante, G. Borzone, A. Perez-Rodriguez, et al., Inorg. Chem. 56, 3467 (2017) (https://doi.org/10.1021/acs.inorgchem.6b03008).

[40] R. Caballero, E. Garcia-Llamas, J.M.M. Merino, M. León, I. Babichuk, V. Dzhagan, et al., Acta Mater. 65 412 (2013) (https://doi.org/10.1016/j.actamat.2013.11.010).

[41] M. Guc, S. Schorr, G. Gurieva, M. Guc, M. Dimitrievska, J. Phys. Energy. 2, 012002 (2020) (https://doi.org/10.1088/2515-7655/ab4a25).

[42] G. Gurieva, D.M.M. Többens, M.Y.Y. Valakh, S. Schorr, J. Phys. Chem. Solids. 99, 100 (2016) (https://doi.org/10.1016/j.jpcs.2016.08.017).

[43] C. Rein, S. Engberg, J.W. Andreasen, J. Alloys Compd. 787, 63 (2019) (https://doi.org/10.1016/j.jallcom.2019.02.014).

[44] A. Khare, A.W. Wills, L.M. Ammerman, D.J. Norris, E.S. Aydil, Chem. Commun. 47, 11721 (2011) (https://doi.org/10.1039/c1cc14687d).

[45] W.C. Liu, B.L. Guo, X.S. Wu, F.M. Zhang, C.L. Mak, K.H. Wong, J. Mater. Chem. A. 1, 3182 (2013) (https://doi.org/10.1039/c3ta00357d).

[46] X. Wang, Z. Sun, C. Shao, D.M. Boye, J. Zhao, Nanotechnology 22, 245605 (2011) (https://doi.org/10.1088/0957-4484/22/24/245605).

[47] B. Flynn, W. Wang, C.H. Chang, G.S. Herman, Phys. Stat. Sol. 209, 2186 (2012) (https://doi.org/10.1002/pssa.201127734).

[48] S.P. Kandare, S.S. Dahiwale, S.D. Dhole, M.N. Rao, R. Rao, Mater. Sci. Semicond. Process. 102, 104594 (2019) (https://doi.org/10.1016/j.mssp.2019.104594).

[49] M.Y. Valakh, V.M. Dzhagan, I.S. Babichuk, X. Fontane, A. Perez-Rodriquez, S. Schorr, JETP Lett. 98, 255 (2013) (https://doi.org/10.1134/S0021364013180136).

[50] Y. Zhao, X. Han, B. Xu, W. Li, J. Li, J. Li, et al., IEEE J. Photovoltaics 7, 874 (2017) (https://doi.org/10.1109/JPHOTOV.2017.2675993).

[51] Y. Jiang, B. Yao, Y. Li, Z. Ding, H. Luan, J. Jia, et al., Mater. Sci. Semicond. Process. 81, 54 (2018) (https://doi.org/10.1016/j.mssp.2018.03.014).

[52] W. Gong, T. Tabata, K. Takei, M. Morihama, T. Maeda, T. Wada, Phys. Stat. Sol. 12, 700 (2015) (https://doi.org/10.1002/pssc.201400343).

[53] A. Ibrahim, A. Guchhait, S. Hadke, H.L. Seng, L.H. Wong, ACS Appl. Energy Mater. 3, 10402 (2020) (https://doi.org/10.1021/acsaem.0c01165).

В. Джаган[1,2], О. Капуш[1], С. Будзуляк[1], Н. Мазур[1], Є. Гаврилюк[1], О. Литвинчук[3], С. Кондратенко[2], В. Юхимчук[1], М. Валах[1]

Колоїдні нанокристали на основі Cu_2ZnSnS_4 леговані Ag: синтез та дослідження методом раманівської спектроскопії

[1]Інститут фізики напівпровідників ім. В.Є. Лашкарьова, Національна академія наук України, Київ, Україна, buser@ukr.net
[2]Національний університет ім. Тараса Шевченка, Київ, Україна, kondratenko@ukr.net
[3]Техаський центр надпровідності і фізичний департамент, Г'юстонський університет, Г'юстон, США litvin@central.uh.edu

Cu_2ZnSnS_4 (CZTS) - один із перспективних матеріалів для поглинаючих шарів тонкоплівкових сонячних елементів нового покоління. В даній роботі розглянуто різні підходи синтезу таких матеріалів з покращеними властивостями та досліджено їх структурні та оптичні характеристики. Варіювання параметрів CZTS (НК) здійснювалося шляхом часткового заміщення катіонів в процесі їх синтезу в колоїдному водному розчині. Зміна параметрів синтезу, зокрема pH розчину, застосовувалась для поліпшення кристалічності НК. Крім того, були успішно синтезовані НК CZTS з частковим заміщенням Cu на Ag. Раманівська спектроскопія використовувалась як основний метод структурної характеристики отриманих НК, поряд із оптичною спектроскопією поглинання та розрахунками динаміки ґратки *ab initio* DFT (Density Functional Theory). В експериментальних раманівських спектрах спостерігається незначний високочастотний зсув характеристичної смуги при збільшенні вмісту Ag в НК $(Ag_xCu_{1-x})_2ZnSnS_4$, що добре узгоджується з розрахунками DFT. Той факт, що даним методом не було отримано чистих Ag_2ZnSnS_4 НК вказує на критичну роль Cu у формуванні структури кестериту в заданих умовах синтезу у водному середовищі.

Ключові слова: CZTS, нанокристали, колоїдний розчин, раманівська спектроскопія, фонони, DFT, сонячні елементи.